Energy Efficient Spike Communication*

David H. Goldberg, Arun P. Sripati, and Andreas G. Andreou
Department of Electrical and Computer Engineering
Johns Hopkins University
3400 N. Charles St., 105 Barton Hall
Baltimore, MD 21218 USA

Abstract

We examine the factors that influence the energy efficiency of communication in spiking neural systems. Our metric of efficiency is the ratio of information rate to power consumption. We formulate quantitative models of spike jitter and power consumption that demonstrate that the number of ion channels participating in spike generation is the key factor that influences energy efficiency. For parameters based on the frog myelinated axon, the energy efficiency has a well-defined optimum. We study the scaling behavior of this optimum and find that the reduction in spike jitter and increase in information rate afforded by more ion channels does not offset the accompanying increase in power consumption.

1 Introduction

Laughlin and co-workers have argued that energy demands of the brain are large enough to have influenced the evolution of neurons, neural codes, and neural circuits [10, 9]. This kind of thinking as led to a new framework by which to study neural systems that couples tools from information theory and bioenergetics to quantify how the brain handles the trade-off between information processing and metabolic demands. In this paper we extend this approach to spike communication.

In spike communication, there is an inherent trade-off between information rate and power consumption. Ion channel stochasticity leads to spike jitter, which limits the information rate of a spiking link. As the number of ion channels is increased, stochasticity is reduced as the random behavior of single channels is averaged out. This reduction in spike jitter leads to an increase in information rate. However, more ion channels mean greater energetic costs associated with maintaining the resting potential and reversing the ionic displacement that occurs during a spike. The information-energy trade-off resulting from signaling with discrete stochastic events was recently examined in [15]. Here, we examine how this trade-off manifests itself in spike communication.

In this work, we quantify the trade-off between information rate and power consumption incurred by spike communication. We define energy efficient behavior as that which maximizes the

*This work was supported by DARPA/ONR contract N00014-00-C-0315.

ratio of information rate to power consumption [3]. We determine the values of spike rate, information rate, and power consumption that correspond to energy efficient performance, and we explore the scaling behavior of the energy efficient optimum. To this end, we develop quantitative models of spike jitter (Sec. 2), information rate (Sec. 3), and power consumption (Sec. 4). We use the frog myelinated axon as the basis for our models, as it is one of the most thoroughly studied spiking links, and experimental measurements of spike jitter are available [8].

2 Spike jitter model

The information rate of a spiking link is limited by the temporal precision of spike occurrences. One measure of spike precision is the standard deviation of the interspike interval distribution, also known as the spike jitter. Schneidman and co-workers demonstrated that the stochasticity of the ion channels near the threshold for spiking gives rise to spike jitter [14]. In order to determine the scaling properties of spike jitter, we require a model that quantitatively expresses this relationship. Additionally, there are few direct measures of spike jitter available in the literature, so a model is useful for estimating spike jitter in various systems.

2.1 Stochastic interval

The key assumption of our spike jitter model is that there is only a brief moment during the rising phase of the action potential when the spike time is vulnerable to ion channel noise. We call this moment the *stochastic interval*. The stochastic interval occurs when the deterministic injected current decreases due to the shape of the action potential at the preceding node and the stochastic Na^+ current takes over as the primary depolarizing current, as shown in Fig. 1(a). From this point on, the value of the Na^+ current can be thought of as a binomial random variable. We can quantify the stochastic nature of the current by looking at the ratio of the instantaneous variance (σ_I^2) to the mean current power (μ_I^2), which we call the noise-to-signal ratio (NSR):

$$\text{NSR} = \frac{\sigma_I^2}{\mu_I^2} = \frac{1-p}{Np} \tag{1}$$

where N is the number of channels and p is the probability of a single channel being open. The stochastic interval is brief because the increasing Na^+ current corresponds to increasing p, and therefore decreasing NSR. This is illustrated in Fig. 1(b), which shows a plot of the NSR superimposed on the action potential shape. There is a well-defined bump in the NSR plot during the rising phase of the action potential that encompasses the putative threshold for spiking. After the bump, the NSR rises again, but the threshold already been surpassed, so this noise does not contribute to the spike jitter.

2.2 From noisy current to spike jitter

Because all phases of the action potential are modeled as deterministic with the exception of the stochastic interval, the variability of the duration of the stochastic interval is equivalent to the

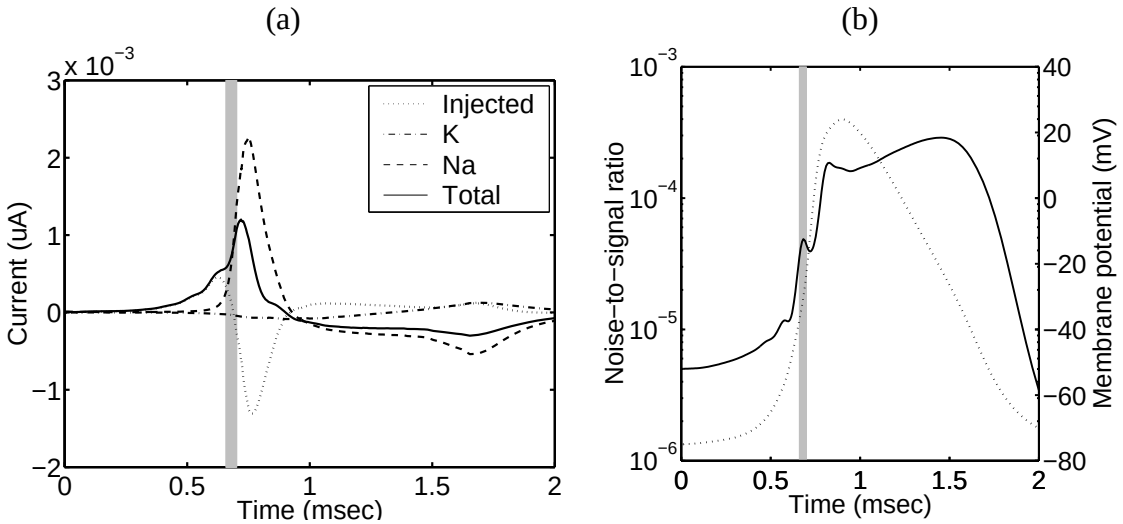

Figure 1: The presence of a stochastic interval in the spiking mechanism of the frog node of Ranvier. The myelinated fiber model is from [6], channel kinetics are based on [7], number of Na^+ channels is $32,000$ [16], and the number of K^+ channels is 28,500 [12]. The 11-node fiber was stimulated at node 1, and the data was recorded at node 6. The last node was shorted to the resting potential. The stochastic interval is indicated by the shaded regions. (a) The currents that contribute to the shape of the action potential. The leakage current was decomposed and absorbed into the other currents. (b) Plot of the ratio of the noise-to-signal ratio (solid line) superimposed on the action potential shape (dotted line). A small constant was added to μ_I^2 to mask zero-crossings of μ_I.

variability of the spike time. The duration of the stochastic interval T is given by

$$T = \frac{C\theta}{I} \tag{2}$$

where C is the capacitance of the node, θ is the range of membrane potentials that define the stochastic interval, and I is current that charges the node capacitance. Because T is short relative to the time constant of the channel noise (determined using the kinetic scheme described in [7] and techniques described in [5]), we model I as constant during one stochastic interval, but as a random variable between stochastic intervals.

This form of the distribution of T was employed by Levine and Shefner to explain the variability of interspike intervals [11]. As discussed in [17], if I is Gaussian, then the distribution of T does not have a finite mean or variance. This problem can be circumvented by describing I with a gamma distribution, which approaches Gaussian as the shape parameter increases. Using this approach, we find

$$\mu_T = \frac{C\theta}{\tilde{\mu}_I} \quad \sigma_T^2 \approx \frac{C^2\theta^2\tilde{\sigma}_I^2}{\tilde{\mu}_I^4} \tag{3}$$

where $\tilde{\mu}_I$ and $\tilde{\sigma}_I^2$ denote the mean and instantaneous variance of the current during the stochastic interval, respectively. This model is attractive because it has the intuitive behavior that the coefficient of variation of the spike time (σ_T/μ_T) is equal to the coefficient of variation of the current (σ_I/μ_I).

2.3 Comparison to experimental data

Using Eq. 3, we can predict the spike jitter that results from ion channel stochasticity in the frog node of Ranvier. Using values of $\tilde{\mu}_I$ and $\tilde{\sigma}_I^2$ from simulation, we find $\sigma_T = [1.16, 6.83]$ μsec for one node. Lass and Abeles measured spike jitter in the frog sciatic nerve [8]. They stimulated the fiber with a pair of fixed-interval pulses and measured the variability of the resulting interspike interval $\sim$10 cm away from stimulation site. They found the standard deviation of the interspike interval σ_{ISI} to be 6 μsec. If we approximate the distribution of T as Gaussian (reasonable for our parameters), then σ_{ISI} and σ_T are related by

$$\sigma_{\text{ISI}} = (2M)^{1/2}\sigma_T \tag{4}$$

where M is the number of nodes that the spike passes through. The factor of 2 in Eq. 4 arises because the variability of the interspike interval encompasses the variability of the starting spike and the ending spike. If we assume an internode distance of 0.14 cm [6], then $M = 72$ nodes. With these parameters, our spike jitter model predicts $\sigma_{\text{ISI}} = [13.9, 82.0]$ μsec. There are several possible explanations for the discrepancy between the predicted and measured values for spike jitter. These include uncertainty in experimental estimates of ion channel counts and our assumption that all of the variability of I occurs between stochastic intervals.

3 Information rate

Spike jitter ultimately limits the degree to which a spiking link can communicate information. We are interested in finding maximum energy efficiency, i.e., the maximum ratio between the information rate and the power consumption. Abeles and Lass showed that a spiking link that employs an interval code with an exponential ISI distribution will communicate more information than a link employing any other code given the same average spike rate [1]. As we will show in the next section, power consumption increases monotonically with spike rate, so the expression for information rate determined with an interval code will give us the highest possible information rate for a given power consumption. Therefore, an interval code is appropriate for our purposes. The expression for information rate, as given in [1], is

$$\text{IR} = \frac{1}{2(t_{\text{ref}} + \frac{1}{\lambda})} \log_2 \left(\frac{e}{2\pi\sigma_{\text{ISI}}^2 \lambda^2} \right) \tag{5}$$

where λ is the spike rate and t_{ref} is the length of the refractory period. We again assume that the distribution of the jitter is Gaussian.

4 Power consumption

Next, we will consider the power consumption of the spiking link. We will consider two principal sources of power consumption: the resting cost and the signaling cost. The resting cost refers to the energy expended by the Na^+-K^+ pumps to maintain the ionic concentration gradients that give rise to the resting potential. The signaling cost refers to the energy used by the pumps to

restore the concentration gradients after they have been perturbed by an action potential. The power consumption (in units of ATP/sec) can be expressed by

$$\mathrm{P} = a\lambda + b \tag{6}$$

where a is the ATP expended per spike, λ is the spike rate, and b is the ATP expended per second due to resting costs.

By considering the stoichiometry of the Na^+-K^+ pump, we find

$$b = \frac{g_{\mathrm{Na}}(V_{\mathrm{rest}} - V_{\mathrm{Na}})}{3e} \tag{7}$$

For the frog node of Ranvier at the resting potential, we have $g_{\mathrm{Na}} = 1.44 \times 10^{-7}$ mS, $V_{\mathrm{rest}} = -75$ mV, and $V_{\mathrm{Na}} = 48$ mV. This gives $b = 3.69 \times 10^7$ ATP/sec/node.

For the calculation of a, we use the approximation of Attwell and Laughlin [2] which states that the number ATP molecules that have to be hydrolyzed to restore resting ionic concentrations following an action potential is one-third of the number of Na^+ ions that have entered the cell. From the frog node of Ranvier simulations described in Sec. 2, we have computed that a net total of 1.93×10^6 Na^+ ions enter the cell during an action potential, corresponding to $a = 6.42 \times 10^5$ ATP/spike/node.

5 The energy efficient optimum

We are interested in the behavior of the spiking link at the energy efficient optimum, i.e. when the ratio between information rate and power consumption is maximized. The energy efficiency (EE) has units of bits/ATP, and we denote the maximum EE as EE^*. Based on the values of σ_{ISI}, a, and b derived in the previous sections (summarized in Table 1(a)), we determine the value of EE^* and the corresponding spike rate, information rate, and power consumption (λ^*, IR^*, and P^*, respectively). We then examine the scaling behavior of EE^*.

5.1 Determination of the optimum

The values of σ_{ISI}, a, and b do not uniquely determine IR and P because they both depend on the spike rate, which is a free parameter. Fig. 2(a) and (b) show IR and P, respectively, as a function of spike rate for the parameters in Table 1(a). The information rate increases monotonically up to the maximum spike rate $1/t_{\mathrm{ref}}$ (Fig. 2(a)). As shown in Fig. 2(b), for low spike rates, the power consumption increases very slowly. As the spike rate increases, the signaling cost ($a\lambda$) surpasses the resting cost (b), and the power consumption increases approximately linearly with spike rate. Fig. 2(c) and (d) plot IR and EE, respectively, versus P. The energy efficiency has a clear maximum, as depicted in Fig. 2(d). The values corresponding to EE^* are denoted by the asterisk on all of the plots and are summarized in Table 1(b).

5.2 Scaling behavior

Next we explore the scaling behavior of the energy efficient optimum. In order to scale the fiber such that voltages and current densities remain constant, we employ the principle of corresponding

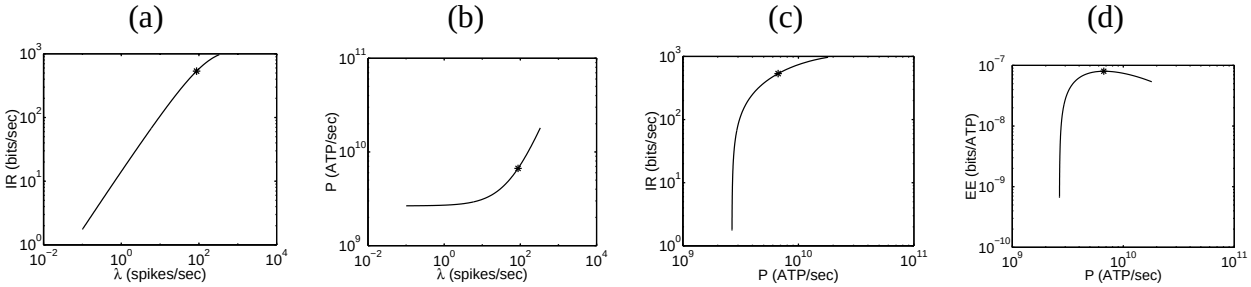

Figure 2: Behavior of the power consumption, information rate, and the energy efficiency. In all of the plots, the point corresponding to the energy efficient optimum is indicated by an asterisk.

(a)

Symbol	Value	Units
σ_{ISI}	35.0	μsec
t_{ref}	3	msec
M	72	nodes
Ma	4.62×10^7	ATP/spike
Mb	2.66×10^9	ATP/sec

(b)

Symbol	Value	Units
λ^*	86.8	spike/sec
P^*	6.67×10^9	ATP/sec
IR^*	534	bits/sec
EE^*	8.01×10^{-8}	bits/ATP

Table 1: (a) Table of parameters derived from the models of Secs. 2 and 4. (b) Values of spike rate, information rate, power consumption and energy efficiency at the energy efficient optimum.

states [13], which dictates that we scale the both fiber diameter and the nodal area by a factor S, while keeping all of the specific properties of the fiber constant.

To determine the scaling behavior of the information rate, we must look at the spike jitter. Because we are keeping the ion channel density, a specific property, constant, the absolute number of ion channels will scale with S. We have

$$C' = CS \quad \mu_I' = \mu_I S \quad \sigma_I' = \sigma_I S^{1/2} \quad \theta' = \theta \tag{8}$$

Therefore, according to Eq. 3,

$$\sigma_T'^2 = \sigma_T^2 S^{-1} \tag{9}$$

As the fiber size increases, the jitter decreases as $S^{-1/2}$. This is an intuitive result, as the more ion channels we have, the more the noise of the individual channels is averaged out. Using Eqs. 5 and 9, we find that as we scale the fiber, the information rate scales as

$$\mathrm{IR}' = \mathrm{IR}\log_2(S) \tag{10}$$

As the fiber gets larger, the jitter gets smaller, and the information rate increases logarithmically.

Using the methods of Sec. 4, we can determine the scaling behavior of the power consumption of the fiber. The number of Na^+ ions that have entered the fiber during an action potential is proportional to I_{Na}, which scales linearly with nodal area and therefore S. The value of b is proportional to g_{Na}, which also increases linearly with nodal area and S. Therefore, we have

$$\mathrm{P}' = (aS\lambda + bS) = \mathrm{P}S \tag{11}$$

We have established that as the fiber scales, information rate grows logarithmically while power consumption grows linearly. These trends alone are not *a priori* sufficient to establish the scaling behavior of EE^* because the spike rate λ is a free parameter. Therefore, for each value of S, we numerically determined EE^*, which in turn gave the values of λ^*, P^*, and IR^*. Plots of λ^*, P^*, IR^*, and EE^* as a function of S are shown in Fig. 3. It turns out that over the values of S we examined, λ^* increases relatively slowly with increasing values of S (Fig. 3(a)). If we approximate λ as constant, it becomes clear that EE^* monotonically decreases with increasing scale factor S, as the denominator P^* grows faster than the numerator IR^* (linearly versus logarithmically), as illustrated in Fig. 3(b)-(d).

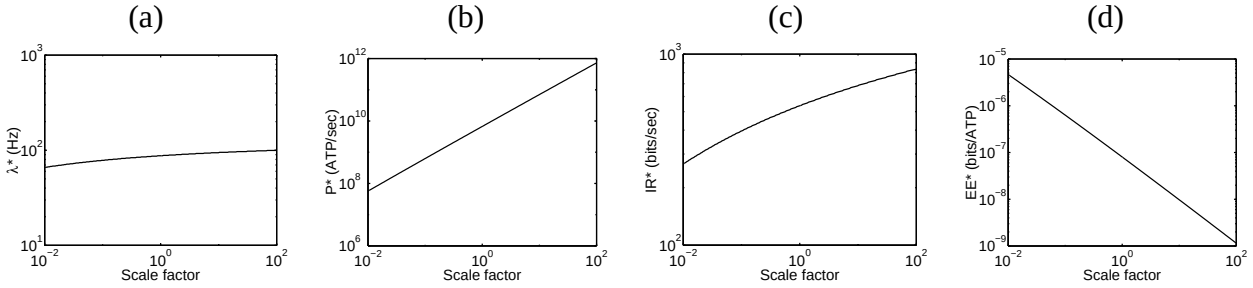

Figure 3: Scaling behavior of the energy efficient optimum in the frog myelinated axon.

6 Discussion

We have examined spike communication in the context of energy efficiency. To this end, we developed quantitative models of spike jitter and power consumption, using the frog myelinated axon as a model system.

We examined the scaling behavior of this system and found that despite the fact that jitter is reduced by increasing the number of ion channels participating in spike generation, the benefits of having more ion channels does not outweigh the accompanying power consumption cost. Because we scaled the system size of the system while maintaining all of the specific properties, our results can be interpreted to mean that for a fixed scale, spiking links should minimize ion channel density in order to realize energy efficient performance.

We have demonstrated that this spiking link has a well-defined optimum with respect to energy efficiency. Our value of the information rate at the optimum energy efficiency is a slightly higher, but still on the same order of magnitude, as information rates measured experimentally [4, Table 2]. Our value of bits per spike at the maximum energy efficiency $\mathrm{IR}^*/\lambda^* = 6.15$ is within the reported range for sensory systems. Laughlin and co-workers estimated a cost of 9×10^5 to 3×10^6 ATP/bit for spike communication in the blowfly large monopolar cell [10]. This compares favorably with our value of $1/\mathrm{EE}^* = 1.25 \times 10^7$. The fact that the energy efficient optimum values for spike rate, information rate, and power consumption are within physiologically plausible ranges support the compelling possibility that energy efficiency may be a guiding constraint in the design of neural systems.

References

[1] M. Abeles and Y. Lass. Transmission of information by the axon: II. The channel capacity. *Biological Cybernetics*, 19:121–125, 1975.

[2] David Attwell and Simon B. Laughlin. An energy budget for signaling in the grey matter of the brain. *Journal of Cerebral Blood Flow and Metabolism*, 21:1134–1145, 2001.

[3] Vijay Balasubramanian, Don Kimber, and Michael J. Berry II. Metabolically efficient information processing. *Neural Computation*, 13:799–815, 2001.

[4] Alexander Borst and Frédéric Theunissen. Information theory and neural coding. *Nature Neuroscience*, 2:947–957, 1999.

[5] Louis J. DeFelice. *Introduction to Membrane Noise*. Plenum Press, New York, 1981.

[6] L. Goldman and J.S. Albus. Computation of impulse conduction in myelinated fibers; Theoretical basis of the velocity-diameter relation. *Biophysical Journal*, 8:596–607, 1968.

[7] B. Hille. Voltage clamp studies on myelinated nerve fibers. In William J. Adelman, Jr., editor, *Biophysics and Physiology of Excitable Membrane*, chapter 12, pages 230–246. Van Nostrand Reinhold, New York, 1971.

[8] Y. Lass and M. Abeles. Transmission of information by the axon: I. Noise and memory in the myelinated nerve fiber of the frog. *Biological Cybernetics*, 19:61–67, 1975.

[9] Simon B. Laughlin. Energy as a constraint on the coding and processing of sensory information. *Current Opinion in Neurobiology*, 11:475–480, 2001.

[10] Simon B. Laughlin, Rob de Ruyter van Steveninck, and John C. Anderson. The metabolic cost of neural information. *Nature Neuroscience*, 1:36–41, 1998.

[11] Michael W. Levine and Jeremy M. Shefner. A model for the variability of interspike intervals during sustained firing of a retinal neuron. *Biophysical Journal*, 19:241–252, 1977.

[12] B. Neumcke, W. Schwarz, and R. Stampfli. Differences between K channels in motor and sensory nerve fibres of the frog as revealed by fluctuation analysis. *Pflugers Archiv*, 387:9–16, 1980.

[13] W.A.H. Rusthon. A theory of the effects of fibre size in medullated nerve. *Journal of Physiology*, 151:101–122, 1951.

[14] Elad Schneidman, Barry Freedman, and Idan Segev. Ion channel stochasticity may be critical in determining the reliability and precision of spike timing. *Neural Computation*, 10:1679–1703, 1998.

[15] Susanne Schreiber, Christian K. Machens, Andreas V.M. Herz, and Simon B. Laughlin. Energy efficient coding with discrete stochastic events. *Neural Computation*, 2002. Submitted.

[16] F.J. Sigworth. The variance of sodium current fluctuations at the node of Ranvier. *Journal of Physiology*, 307:97–129, 1980.

[17] Charles E. Smith. A comment on a retinal neuron model. *Biophysical Journal*, 25:385–386, 1979.